CLM-P 106

United Kingdom Atomic Energy Authority

RESEARCH GROUP

Preprint

ELECTRON CYCLOTRON INSTABILITY EXPERIMENT

D. L. MORSE

Culham Laboratory,

Culham, Abingdon, Berkshire

1966

UNCLASSIFIED
(Approved for Publication)

CLM - P 106

ELECTRON CYCLOTRON INSTABILITY EXPERIMENT

by

D.L. MORSE

(Submitted for publication in J. Nucl. Energy Pt.C)

A B S T R A C T

Electrostatic oscillations are excited in a cylindrical shell of plasma by an electron beam which passes through the plasma with a helical trajectory. A non-convective instability results in an unstable wave which propagates in the same azimuthal direction, and in the opposite axial direction, as the electron beam. The qualitative behaviour of the instability is in agreement with the theoretical predictions, and the frequency and wavelength of the unstable wave agree with calculated values to within 25%.

U.K.A.E.A. Research Group,
Culham Laboratory,
Nr. Abingdon,
Berks.

June, 1966 (MEA)

CONTENTS

1. INTRODUCTION

In the study of plasma microinstabilities, there has been much recent interest in instabilities excited by anisotropic velocity distributions of one or more of the species of plasma particles. The experiment described in this paper is concerned with the excitation of such an instability under controlled conditions, and the study of its properties.

Instabilities arising from velocity-space anisotropies have been studied theoretically by CRAWFORD and TATARONIS (1965), DNESTROVSKY et al. (1963), GRUBER et al. (1965), HALL et al. (1965), NEUFELD and WRIGHT (1964), ROSENBLUTH and POST (1965), and SOPER and HARRIS (1965). The theory which most closely approximates the experiment described here is that of BURT and HARRIS (1961). These authors considered electrostatic oscillations of a cylindrical shell of plasma excited by ions gyrating in cyclotron orbits concentric with, and of the same diameter as, the plasma shell. In the experiment described here, the gyrating ions are replaced by electrons and these electrons have a small axial drift velocity in addition to their gyratory motion.

The system has been analysed theoretically by CORDEY (1965), and it is found that unstable electrostatic oscillations will occur for certain ranges of electron cyclotron frequency, plasma electron density, and density of the gyrating electrons. The theoretical predictions are compared with the experimental results in section 5.

2. EXPERIMENTAL APPARATUS

A schematic diagram of the experimental configuration is shown in Fig.1. The instability takes place in the annular region bounded on the outside by the outer tube and on the inside by the cold trap. The system is immersed in an axial magnetic field of 30 to 60 gauss. The cold trap maintains a neutral pressure of mercury vapour of about 1×10^{-5} torr.

The plasma is generated by a mercury arc source located about one meter below the experimental region shown in Fig.1. Plasma is conducted along the magnetic field to the plate shown in the bottom of Fig.1, and then streams through the defining slot in the annular shape shown. The plasma density in the region shown may be adjusted in the range 3×10^{7} to 10^{9} cm^{-3} by varying the current to the outer edge of the defining slot.

To generate the cylindrical shell of gyrating electrons, an electron beam is fired into the plasma at an angle of about 6^{o} from the horizontal. The beam current is generally

between 1 and 3 mA. The beam voltage lies between 1500 and 6500 volts, and is adjusted as the magnetic field is varied to keep the cyclotron radius of the beam electrons the same as the radius of the plasma annulus.

The electron beam spreads axially from the ribbon shape shown in Fig.1 to form a hollow cylinder of gyrating electrons of density 1 to 3 $\times$ 10^6 cm^{-3}. The axial density profile of the beam is shown in Fig.2. This profile is taken one-quarter of a revolution from the position of the electron gun, so the first peak in density at the right of the figure represents the axial profile of the beam after it has travelled one-quarter of a revolution from the gun. The changes in pitch of the beam helix are due to small variations in the axial magnetic field strength.

From Fig.2 the average axial spreading velocity of the beam is deduced to be approximately 4 $\times$ 10^7 cm sec^{-1}, equivalent to an axial "thermal" energy of about one-half of an electron volt. This axial "thermal" velocity is an important parameter, since it determines the minimum axial phase velocity at which waves may propagate without Landau damping. The spreading velocity may be partly of thermal origin, since the gun cathode is directly-heated tantalum running at approximately 2000^{o}K, but, probably, is mainly due to incomplete neutralization of the beam. The axial spreading has been observed to decrease at higher neutral pressure, when the beam is more completely neutralized.

The strongest radio frequency oscillations from the instability are received in the axial region between approximately 7 and 15 cm in Fig.2. In this region, which we call the "interaction region", the axial spreading of the beam electrons has changed the beam from its helical ribbon shape to a reasonably uniform hollow cylinder of electrons.

In Fig.3 typical radial density profiles of the beam and plasma in the interaction region are shown, again at an azimuthal position one-quarter of a revolution from the electron gun. The beam has its widest radial spread at this position and at three-quarters of a revolution from the gun, while it is best focused radially one-half of a revolution from the gun and directly underneath it. At one-half of a revolution from the gun, the peak beam density is about twice as great as at one-quarter of a revolution and the profile is proportionately sharper. For the remainder of this paper, the beam density referred to will be that measured in the interaction region at an azimuthal position one-quarter of a revolution from the gun. The beam density is usually less than 1% of the plasma density and rises to about 3% in extreme cases.

The peak beam density occurs at a radius somewhat smaller than the mean radius of the annulus, to coincide with the radius of the peak plasma density. The latter is nearer the cold trap than the outer wall because the plasma is generated on the system axis and its density is greater near the inner edge of the defining slot than near the outer edge. The peak plasma density varies by about 20% around the annulus at a fixed axial position, and decreases by about 20% over the length of the interaction region from bottom to top. All plasma density measurements are made with a cylindrical Langmuir probe, and the current-voltage characteristics interpreted using the curves published by CHEN (1965).

The axial thermal velocity of the plasma electrons is estimated using a disc-shaped Langmuir probe. The axis of the disc, normal to its surface, is oriented parallel to the magnetic field and the collecting surface of the disc faces the plasma defining slot. From the electron-collection part of the probe characteristics, the axial thermal velocity of the plasma electrons is found to be approximately 6×10^7 cm sec^{-1} corresponding to a thermal energy of one electron volt.

The electrostatic oscillations resulting from the instability are detected with a VHF communications receiver of 5 microvolt sensitivity, connected to any one of a number of antennas located near the outer tube wall in the interaction region. Each antenna is a simple dipole type, oriented parallel to the axis of the system.

The wavelength of the instability is measured by summing the signals from two antennas and feeding the summed signal to the receiver. When the antennas are $(n + \frac{1}{2})$ wavelengths apart (either axially or azimuthally) the summed signal is minimized. When they are n wavelengths apart, the signal is maximized. Several antennas are placed around the perimeter of the tube at a fixed axial position for measuring the azimuthal wavelength and an antenna, movable axially at a fixed azimuthal position, is used to measure the axial wavelength. This system of wavelength measurement is sensitive only to a travelling wave. No axial or azimuthal standing wave pattern has been observed in any of the experiments.

The axial direction of propagation of the wave is measured in the following way. The axial position of the movable antenna is adjusted so that the sum of its signal with the signal from a fixed antenna is minimized. A short length of cable is added between the summation point and the movable antenna, and the position of the antenna readjusted for a minimum summed signal. Since the short length of cable retards in phase the signal to the summation point, to regain the minimum the antenna must be moved to compensate for this, counter to the direction of wave propagation. Hence the direction in which the antenna is

moved is opposite to the axial direction of propagation. The azimuthal direction of propogation is found in an analogous way, except that successive antennas spaced around the perimeter of the tube are used in place of the movable antenna.

3. THEORY

The theory of CORDEY (1965) has been used to predict the ranges of parameters over which unstable electrostatic oscillations may be excited. The following assumptions, among others, are made:

(i) The beam and plasma uniformly fill the region between two infinitely long, coaxial, conducting cylinders of radius r_1 and r_2. The thickness of the region $a = r_2 - r_1$ is assumed to be small compared with r_1. The z-axis is taken along the axis of the cylinders.

(ii) An axial magnetic field is applied parallel to the z-axis.

(iii) The plasma ions remain stationary and serve only to preserve average charge neutrality.

(iv) The effect of all collisions is neglected.

Assuming a time- and space- dependence of the form $e^{-ikz - i\ell\theta + i\omega t}$, the following dispersion relation is derived:

$$\lambda^2 \left\{ 1 + \omega_{pb}^2 \int_{-\infty}^{\infty} \frac{f_b(v)dv}{\omega_{ce}^2 - (\omega - \ell\omega_{ce} - kv)^2} + \omega_{pe}^2 \int_{-\infty}^{\infty} \frac{f_p(v)dv}{\omega_{ce}^2 - (\omega - kv)^2} \right\}$$

$$+ k^2 \left\{ 1 - \omega_{pb}^2 \int_{-\infty}^{\infty} \frac{f_b(v)dv}{(\omega - \ell\omega_{ce} - kv)^2} - \omega_{pe}^2 \int_{-\infty}^{\infty} \frac{f_p(v)dv}{(\omega - kv)^2} \right\} = 0 \qquad \ldots (1)$$

In this equation, ω_{pe} is the plasma frequency of the plasma electrons, ω_{pb} is the plasma frequency of the beam electrons, ω_{ce} is the electron cyclotron frequency, ω is the oscillation frequency, $\lambda = \pi/a$ is the radial wave number, ℓ is the azimuthal mode number (an integer), k is the axial wave number, v is the axial velocity, and $f_p(v)$ and $f_b(v)$ are the plasma and beam axial distribution functions respectively.

Both the Maxwellian distribution and the Lorentzian distribution were used for $f_p(v)$ and $f_b(v)$, and the results found to be very similar. For the computed results given in this paper, the Lorentzian distribution was used:

$$f_p(v) = \frac{1}{\pi} \frac{v_{tp}}{v^2 + v_{tp}^2} \qquad \ldots (2)$$

$$f_b(v) = \frac{1}{\pi} \frac{v_{tb}}{(v-v_o)^2 + v_{tb}^2} . \qquad \ldots (3)$$

In these definitions, v_{tp} and v_{tb} are the axial thermal velocities of the plasma and beam electrons respectively, and v_o is the average axial drift velocity of the beam electrons.

Using the criterion of BERS and BRIGGS (1964), a non-convective instability is found whose azimuthal direction of propogation is the same as that of the gyrating beam electrons ($\ell = +1$) and whose axial direction of propogation is opposite to v_o ($kv_o < 0$). The experimental results are compared with the predicted behaviour of this instability in section 5. The theory further predicts a convective instability when $\ell = +1$ and $kv_o > 0$, and instabilities for $\ell = 2,3, \ldots$ at higher plasma densities, but these have not been observed.

To gain insight into the nature of the instability, it is instructive to look at the dispersion characteristics of the beam and plasma waves separately. These are given in Fig.4 for $\ell = +1$ and no thermal motion of the beam and plasma electrons. The solid lines represent the well-known dispersion characteristics of a waveguide filled with stationary plasma, assuming $\omega_{pe} > \omega_{ce}$ (CHORNEY, 1958; TRIVELPIECE and GOULD, 1959). The dashed lines represent the beam waves, which couple to the plasma waves at the intersections of the dispersion curves.

The instability reported here arises from the coupling between the beam and plasma waves in region A of Fig.4. The beam wave in this region may be shown by the method of BERS and GRUBER (1965) to carry negative energy, and hence its coupling to the plasma wave results in an instability. The frequency of the unstable oscillations will be slightly below $\omega_{ce} + kv_o$, with $k < 0$.

A physical explanation of the mechanisms of the various types of cyclotron instability is given by HALL et al. (1965). In our experiment, the electric field of the plasma wave has both an axial and an azimuthal wave number. The axial component of this field leads to a bunching of the beam electron density in both the axial and azimuthal directions, and energy is extracted from the bunched beam electrons due to their retardation by the azimuthal electric field of the plasma wave.

Some of the qualitative features of the theoretical predictions are given below:

(i) The frequency of oscillation ω will be slightly below the Doppler-shifted cyclotron frequency, $\omega_{ce} + kv_o$. Since $kv_o < 0$, ω will lie below ω_{ce}. The oscillation frequency ω will always be less than ω_{pe}.

(ii) If ω_{pb} and ω_{ce} are held fixed and ω_{pe} increased from zero, the instability will appear when ω_{pe} exceeds a lower limit which is less than ω_{ce}.

(iii) As ω_{pe} is increased above the lower limit for instability, ω will increase relatively rapidly with ω_{pe} until ω_{pe} is somewhat greater than ω_{ce}. Since $\omega \approx \omega_{ce} + kv_o$ and $kv_o < 0$, an increase in ω implies an increase in the axial wavelength.

(iv) As ω_{pe} is increased further above ω_{ce}, ω and k remain approximately constant.

(v) For sufficiently large ω_{pe}, the instability is quenched.

(vi) If ω_{pb} is fixed, there is a lower limit of ω_{ce} below which no $\ell = 1$ instability occurs for any value of ω_{pe}.

In the next two sections the experimental results are given and compared with the predictions of the theory.

4. EXPERIMENTAL RESULTS

A typical set of experimental results is shown in Fig.5. The oscillation frequency spectrum and axial wavelength are plotted as a function of plasma density, at constant magnetic field and beam density. Each of the qualitative predictions (i) to (v) of the previous section is exhibited by these results.

The band of unstable frequencies vs. plasma density is shown in the right hand side of Fig.5, where the x's denote the frequency of the strongest oscillation at a particular plasma density. At this value of magnetic field, the oscillation frequency makes discontinuous jumps around f_{pe} = 125 Mc/s and 165 Mc/s. The origin of this behaviour is not understood, and for the remainder of this paper only the gross features of the spectrum are compared with the theory.

Using the measured values of the axial wavelength and the axial beam velocity, the difference between the oscillation frequency and the Doppler-shifted cyclotron frequency can be calculated. For the set of results shown in Fig.5, the oscillation frequency is displaced between 2 and 10 Mc/s below the Doppler-shifted cyclotron frequency, and the average displacement is 6 Mc/s.

In all of the experiments, the axial direction of propogation is found to be opposite to the axial beam velocity, and the azimuthal direction of propogation is the same as the gyrating beam electrons. The azimuthal mode number is always found to be $\ell = +1$. The higher azimuthal modes, which the theory predicts become unstable at higher plasma densities, have not been observed.

5. COMPARISON BETWEEN EXPERIMENT AND THEORY

(i) AXIAL WAVELENGTH VS. PLASMA DENSITY

The measured variation of axial wavelength with plasma density is compared with theory in Fig.6 for two different values of electron cyclotron frequency f_{ce}. The comparisons for f_{ce} = 141 Mc/s and 94 Mc/s represent respectively the best and poorest agreement between the experimental and theoretical wavelengths. The theoretical wavelengths are generally shorter than the experimental ones, and the poorest agreement occurs at higher plasma densities. The discrepancy is less than 25% of the computed wavelength.

(ii) OSCILLATION FREQUENCY SPECTRA VS. PLASMA DENSITY

The measured and computed oscillation frequency spectra vs. plasma density at f_{ce} = 110 Mc/s are compared in Fig.7. As in Fig.5, the x's denote the frequency of strongest oscillation at a given plasma density. The computed frequencies are Doppler-shifted farther below f_{ce} than the experimental ones at a given density, consistent with the shorter computed axial wavelengths. The discrepancy between the measured and computed frequencies is generally less than 10%, and is smaller at larger values of f_{ce}.

In Fig.7 we have compared the measured spectrum at a beam plasma frequency f_{pb} of 15 Mc/s with the computed spectrum at f_{pb} = 10 Mc/s. A weaker beam is necessary in the theory because the beam is assumed to uniformly fill the region between the cold trap and the outer wall, whereas in practice the beam fills only a small part of this region. The theoretical value of f_{pb} = 10 Mc/s is chosen to be equivalent to a measured value of 15 Mc/s because it is found that with these values of f_{pb} the computed and measured displacement of the frequency spectrum below the Doppler-shifted cyclotron frequency are approximately equal. Theory predicts that this displacement is a function of the beam density.

Fig.7 also shows that at f_{ce} = 110 Mc/s the theoretical lower limit of plasma density for unstable oscillations is lower than the experimental value. This is true for all values of magnetic field investigated. The theoretical and experimental upper density limits are

in good agreement at f_{ce} = 110 Mc/s, but for stronger magnetic fields the experimental limit generally lies below the theoretical limit. The strongest oscillations occur when $f_{pe} \approx f_{ce}$. The theory predicts the largest growth rates for the instability when this condition is approximately satisfied.

(iii) STABILITY BOUNDARIES IN THE MAGNETIC FIELD - PLASMA DENSITY PLANE

Fig.8 shows the upper and lower plasma density limits for instability vs. magnetic field, for several values of beam density. The locus of the limits for a given beam density constitutes a stability boundary in the magnetic field - plasma density plane. The experimental boundaries are compared with theoretical ones calculated for f_{pb} = 7 Mc/s and 10 Mc/s.

The theoretical upper limits of plasma density for unstable oscillations lie above the measured limits for the larger values of magnetic field. The computed e-folding growth time in the plasma density range between the theoretical and experimental upper limits is greater than 0.1 microsecond. It is therefore possible that the measured upper limit is lowered due to damping by electron-neutral collisions, whose frequency is approximately 1 Mc/s.

As noted previously, the theoretical lower limits of plasma density for unstable oscillations lie below the measured limits throughout the range of magnetic field. This discrepancy may be due to the inhomogeneity of the plasma. Since the plasma does not uniformly fill the region between the cold trap and the outer tube as assumed by the theory, it is possible that it has a lower effective density than the peak density measured by the Langmuir probe. In any case Fig.8 shows that the computed lower limits of f_{ce} for which no unstable oscillations occur for any value of plasma density agree well with the measured values.

6. CONCLUSIONS

Unstable electrostatic oscillations in a cylindrical shell of plasma have been excited by electrons gyrating in cyclotron orbits through the plasma shell. The measured properties of the instability are found to be in good qualitative agreement with theory. In the range of parameters investigated, the discrepancies between theory and experiment are no worse than the following percentages of the theoretical values:

Oscillation frequency : 10%
Axial wavelength : 25%
Plasma frequency at stability boundary : 50%.

7. ACKNOWLEDGEMENTS

The author would like to express his appreciation to Dr. P.C. Thonemann for the original conception of the experiment and for suggestions and encouragement during the experimental program. Many aspects of the design of the experimental apparatus are due to the efforts of Dr. G.C. Thomas. Dr. J.G. Cordey contributed many helpful suggestions concerning the interpretation of the experimental results, and performed all the numerical computations. The assistance of W.H.W. Fletcher and N.R.G. Ainsworth in the construction, maintenance, and operation of the experiment is gratefully acknowledged.

8. REFERENCES

1. BERS, A. and BRIGGS, R.J. (1964), Massachusetts Institute of Technology, Research Laboratory of Electronics, Quarterly Progress Report No.71, 122.

2. BERS, A. and GRUBER, S. (1965), Appl. Phys. Letters 6, 27.

3. BURT, P. and HARRIS, E.G. (1961), Physics Fluids 4, 1412.

4. CHEN, F.F. (1965), Plasma Physics (J. Nucl. Energy, Pt.C) 7, 47.

5. CHORNEY, P. (1958), Massachusetts Institute of Technology, Research Laboratory of Electronics, Technical Report No.277.

6. CORDEY, J.G. (1965), United Kingdom Atomic Energy Authority Research Group Report CLM - R 44

7. CRAWFORD, F.W. and TATARONIS, J.A. (1965), J. Appl. Phys. 36, 2930.

8. DNESTROVSKY, Yu. N., KOSTOMAROV, D.P. and PISTUNOVICH, V.I. (1963), Nucl. Fusion 3, 30.

9. GRUBER, S., KLEIN, M.W. and AUER, P.L. (1965), Physics Fluids 8, 1504.

10. HALL, L.S., HECKROTTE, W. and KAMMASH, T. (1965), Phys. Rev. 139, A 1117.

11. NEUFELD, J. and WRIGHT, H. (1964), Phys. Rev. 135, A 1175.

12. ROSENBLUTH, M.N. and POST, R.F. (1965), Physics Fluids 8, 547.

13. SOPER, G.K. and HARRIS, E.G. (1965), Physics Fluids 8, 984.

14. TRIVELPIECE, A.W. and GOULD, R.W. (1959), J. Appl. Phys. 30, 1784.

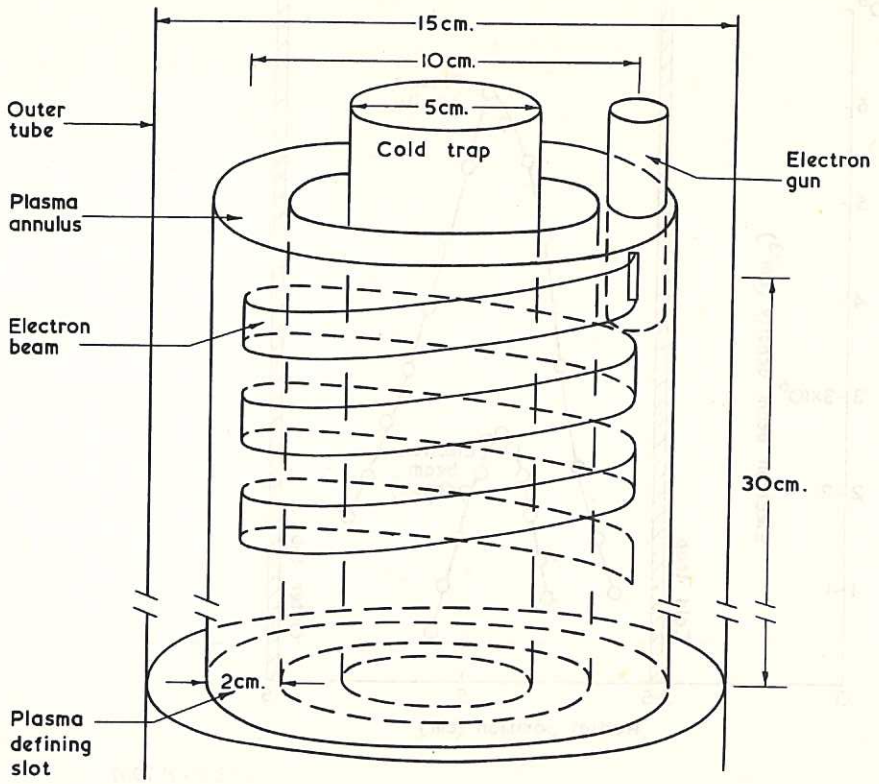

Fig. 1 Experimental configuration (CLM-P106)

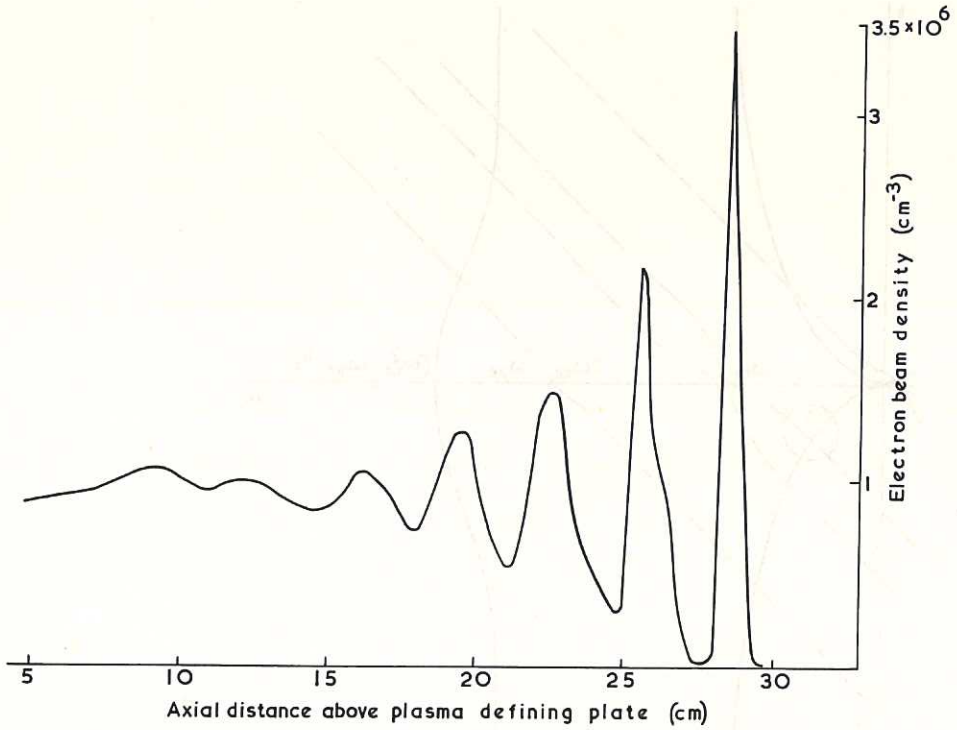

Fig. 2 (CLM-P106)

Electron beam axial density profile :- Magnetic field : 39 gauss:
Beam voltage : 3600 volts; Beam current : 1 mA

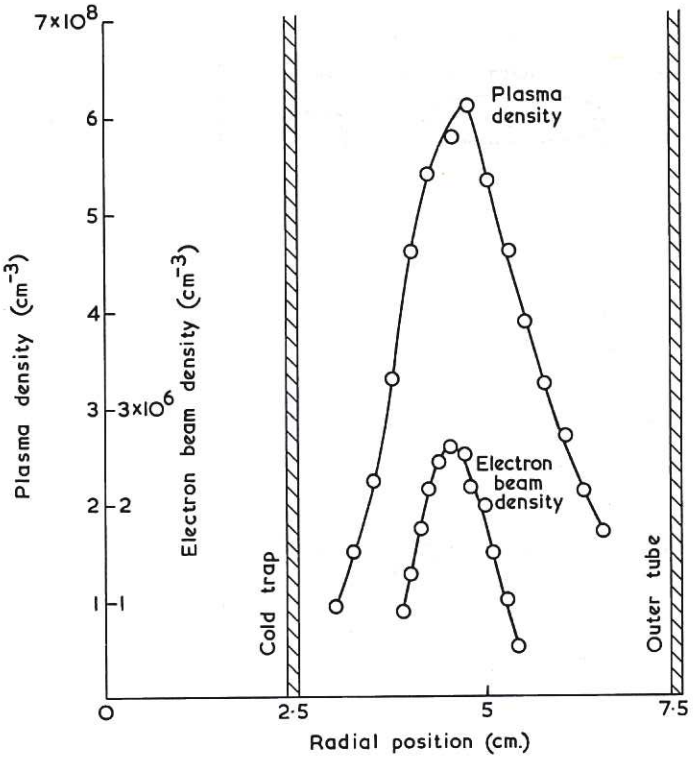

Fig. 3 (CLM - P 106)

Typical beam and plasma radial density profiles :- Magnetic field : 39 gauss : (Note different scales for beam and plasma density)

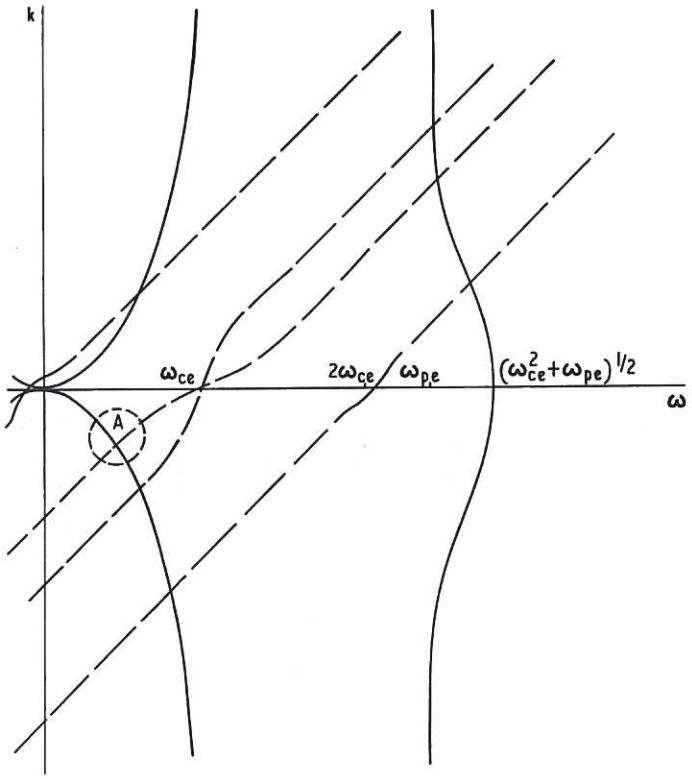

Fig. 4 (CLM - P 106)

Dispersion characteristics of electrostatic waves in plasma and electron beam. Solid lines : plasma waves. Dashed lines : beam waves. Asymptotic slope of beam wave curves is v_o^{-1}. Coupling in region A gives rise to instability reported here.

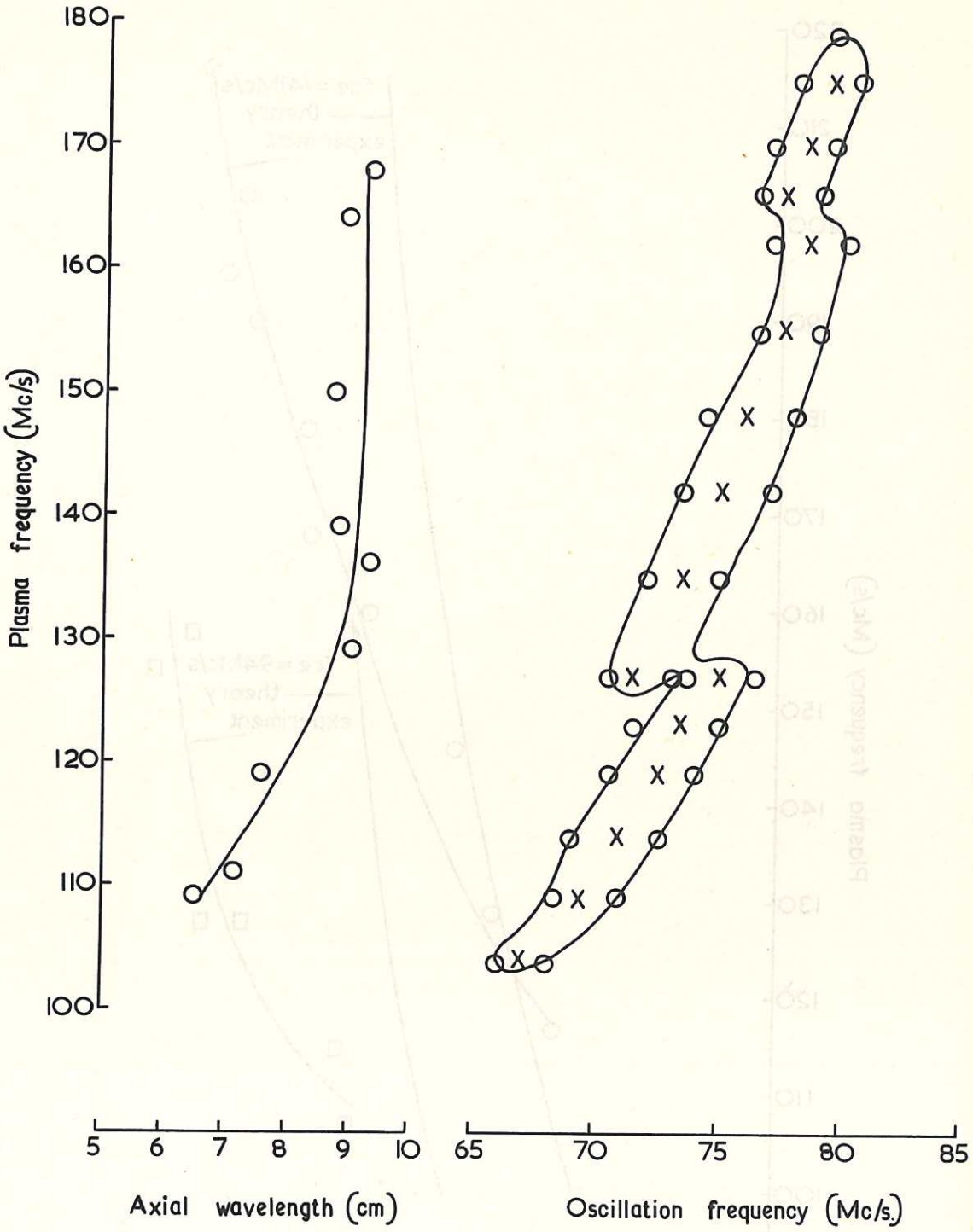

Fig. 5 (CLM - P 106)

Oscillation frequency and axial wavelength vs. plasma density :
Electron cyclotron frequency : 110 Mc/s
Beam plasma frequency : 12.5 Mc/s

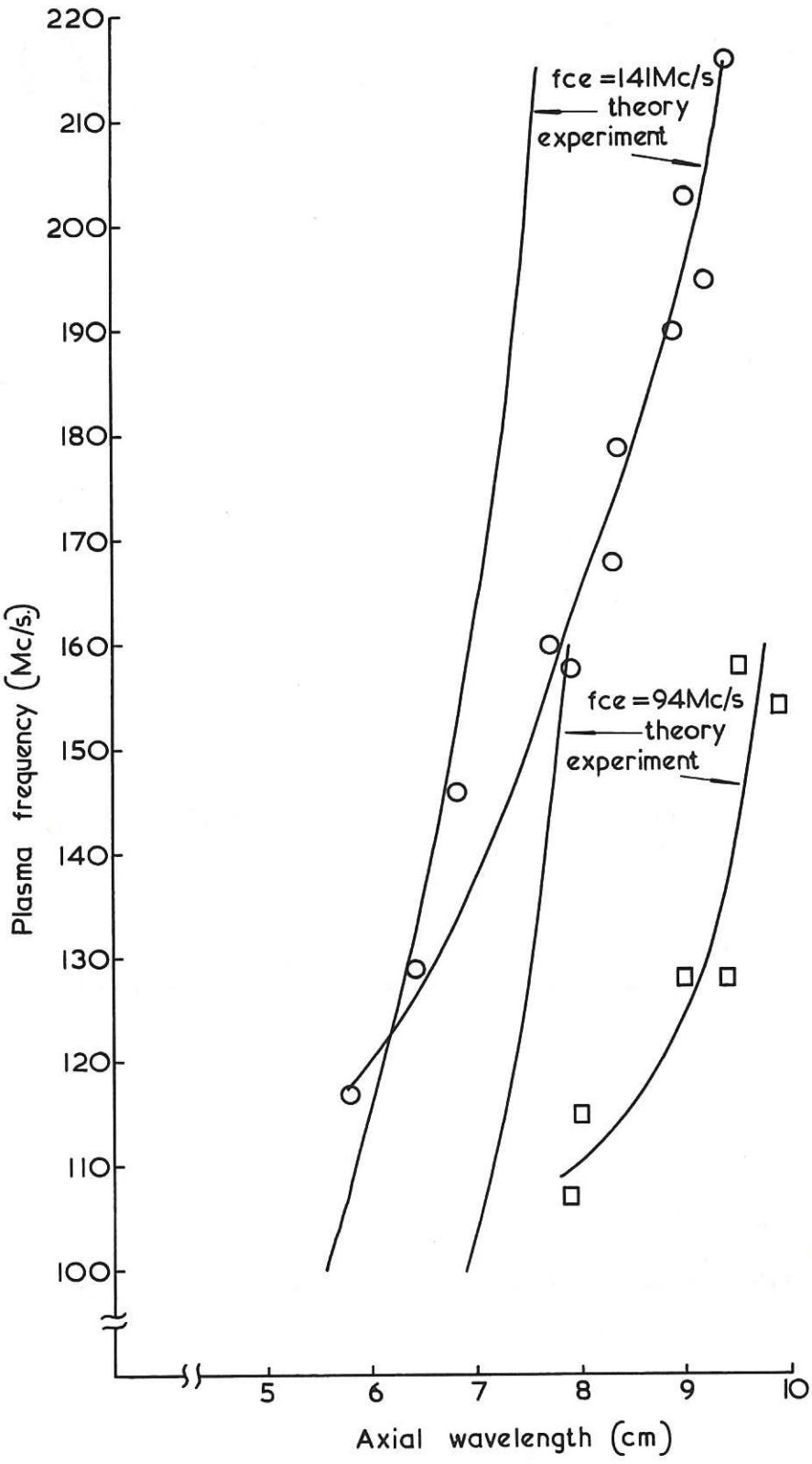

Fig. 6 (CLM-P 106)
Measured and computed axial wavelength vs. plasma density:
Beam plasma frequency: 15 Mc/s

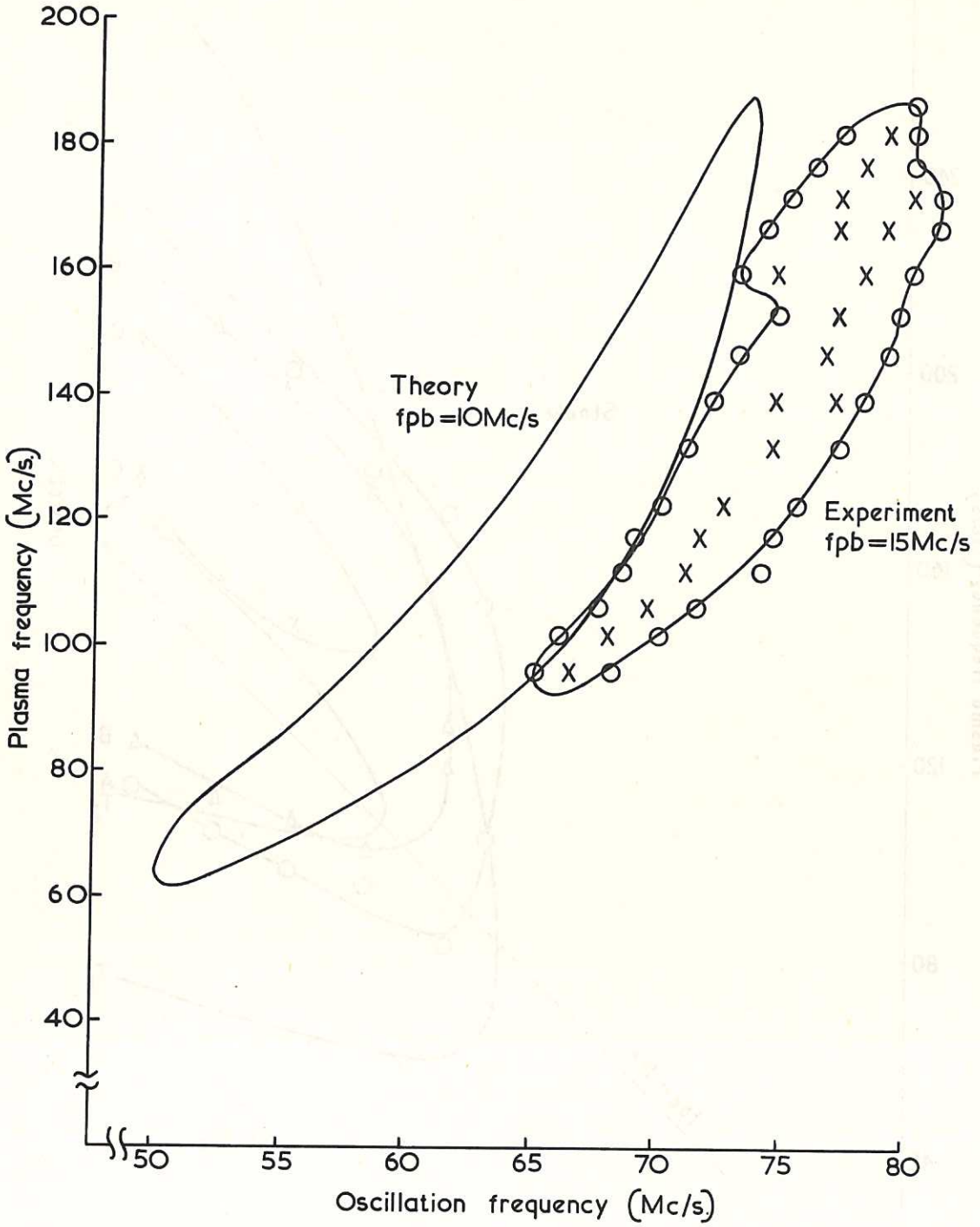

Fig. 7 (CLM-P 106)
Measured and computed frequency spectra vs. plasma density:
Electron cyclotron frequency: 110 Mc/s

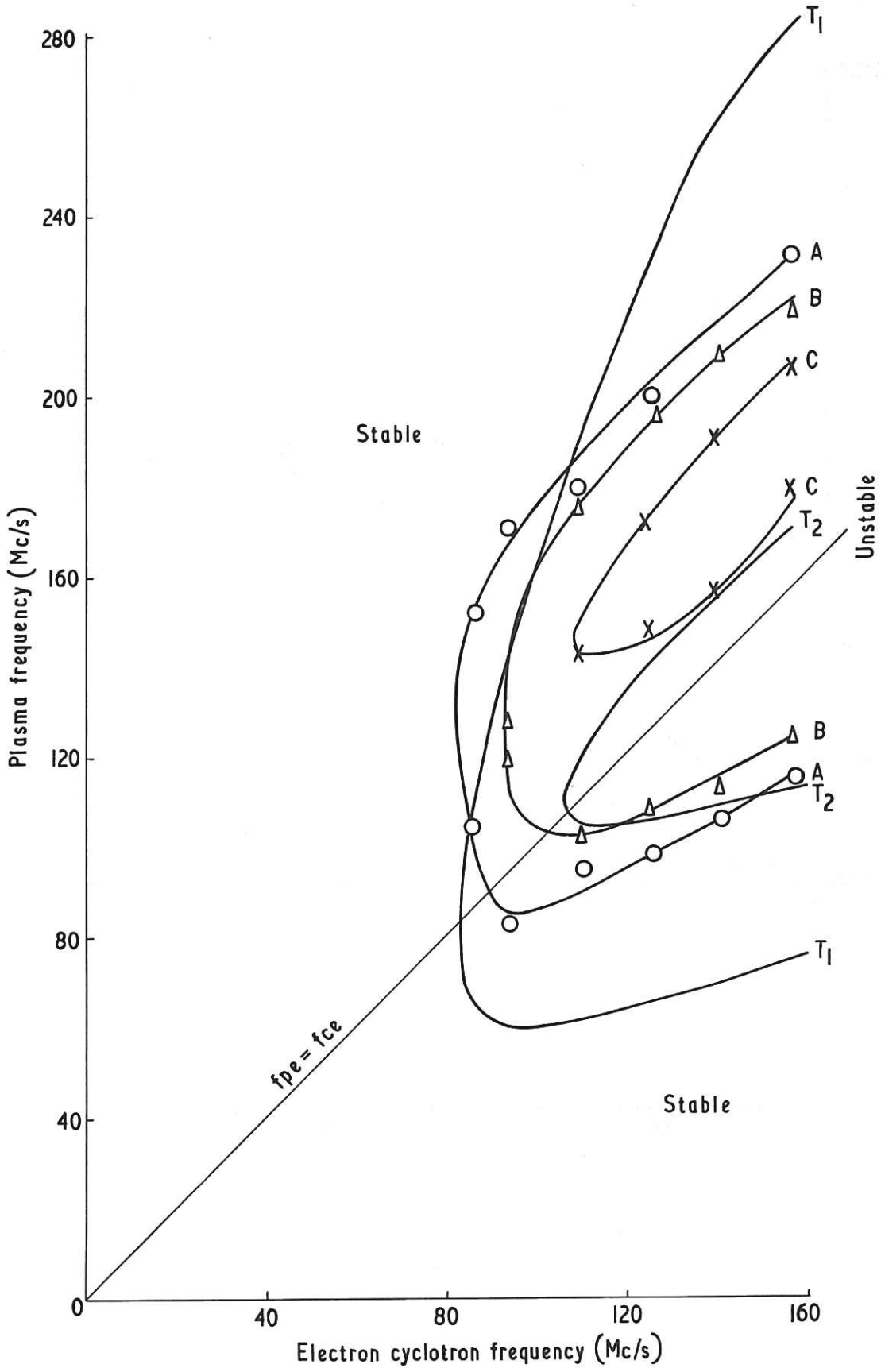

Fig. 8 (CLM - P 106)

Experiment and theoretical stability boundaries in the magnetic field - plasma density plane. Beam plasma frequency (experimental curves) A, 15 Mc/s; B, 12.5 Mc/s; C, 10 Mc/s: (theoretical curves) T_1, 10 Mc/s; T_2, 7 Mc/s